which is very similar to the rate by Coble, compares well with the lattice diffusion model by Herring, and agrees with experimental results.[7]

If the grain size is approximately an order of magnitude larger than the thickness within which diffusion is enhanced, Eq. (12) provides very good agreement with experimental results.[7] If the grain sizes are on the order of the apparent widths of boundaries deducted from measurements, the lattice model[1] should be used.

Conclusions

A boundary diffusion controlled creep model for nanocrystals based on existing models and theories has been developed. In the spherical analog for the vacancy source, the boundary of rotational symmetry between equal areas was taken to be 45 deg below the nanocrystalline pole (see Fig. 3). It is at 45 deg that the maximum flux exists. The proportionality constant N and the creep rate compare well with other studies. It is agreed that creep control is more successful by boundary diffusion when it takes place at larger grain sizes and smaller interfacial components.

References

[1]Herring, C., "Diffusional Viscosity of a Polycrystalline Solid," *Journal of Applied Physics*, Vol. 21, No. 5, 1950, pp. 437–445.

[2]Coble, R. L., "A Model for Boundary Diffusion Controlled Creep in Polycrystalline Materials," *Journal of Applied Physics*, Vol. 34, No. 6, 1963, pp. 1679–1682.

[3]Coffey, C. S., "A Prototypical Model of a Dislocation Source Capable of Generating Shear Band Structures in Crystalline Solids During Shock or Impact," *Journal of Applied Physics*, Vol. 66, No. 4, 1989, pp. 1654–1657.

[4]Nieman, G. W., Weertman, J. R., and Siegel, R. W., "Properties of Nanocrystalline Palladium," Scripta Metallurgica et Materialia, Vol. 24, 1989, pp. 145–150.

[5]Birringer, R., "Nanocrystalline Materials," *Materials Science and Engineering*, Vol. A117, 1989, pp. 33–43.

[6]Gryaznov, V. G., Solovev, V. A., and Trusov, L. I., "The Peculiarities of Initial Stages of Deformation in Nanocrystalline Materials," *Scripta Metallurgica et Materialia*, Vol. 24, 1990, pp. 1529–1534.

[7]Paladino, A. E., and Coble, R. L., "Effect of Grain Boundaries on Diffusion-Controlled Process in Aluminum Oxide," *Journal of the American Ceramic Society*, Vol. 46, No. 3, 1963, pp. 133-136.

Elastodynamic Characteristics of Hollow Cantilever Beams Containing an Electrorheological Fluid: Experimental Results

Seung-Bok Choi* and Yong-Kun Park†
Inha University, Incheon 402-751, Republic of Korea
and
Moon-Suk Suh‡
Agency for Defense Development, Taejon 305-600, Republic of Korea

Introduction

THE vibration control of flexible structures with variable disturbances in different frequencies becomes more and more important because of the demand for higher positional accuracy and more stable manipulation. To achieve this goal, the resonance of the structures must be avoided in all cases. For traditional structures, the frequencies of the disturbances must be known and guessed before the design of the structures to avoid the excitations imposed in the neighborhood of the structural natural frequencies. For variable excitations, this methodology cannot be adopted. However, smart material structures that have their own sensing, actuating, tuning, controlling, and computational capabilities can be adjusted to variable disturbances. Typically, smart materials and structures[1] are employed to control the static and elastodynamic responses of distributed parameter systems. This may be accomplished by controlling the mass distribution, stiffness characteristics, and energy dissipation characteristics of the structure. Recently, significant progress has been made in the development of smart materials and structures that incorporate piezoelectric materials,[2] shape memory alloy,[3] and electrorheological (ER) fluids.[4]

This paper reports on a proof-of-concept experimental investigation focused on evaluating the elastodynamic characteristics of hollow cantilever beams filled with a hydrous-based ER fluid consisting of cornstarch and silicone oil. The beams are considered to be uniform viscoelastic materials and modeled as a viscously damped harmonic oscillator. Electric-field-dependent natural frequencies, loss factors, and complex moduli are evaluated and compared among three different beams: two types of different volume fraction of the ER fluid and one type of different particle concentration of the ER fluid by weight. It is also shown that, by tailoring the electric field, structural resonances can be avoided to provide the feasibility of active vibration control applications under unstructured environmental conditions.

Experimental Apparatus and Procedures

The structure of the proposed beam specimen shown in Fig. 1 consists of two faceplates, rubber and acrylic. The faceplates can act as electrodes, and the rubber serves as a seal to hold the integrity of the specimen. The specifications of the ER fluid and three specimens used in this study are presented in Table 1. The cantilever specimen was clamped in a fixture that was bolted down on top of the shaker head as shown in Fig. 2. A noncontacting probe was mounted near the tip of the specimen to pick up the vibration responses. In forced vibration, the damped natural frequencies with respect to the electric field were measured through the fast Fourier transform (FFT) analyzer by sweeping the sine wave from 0 to 100 Hz.

In free vibration, by assuming that the first mode is dominant and that the material is uniform and viscoelastic, we modeled the specimen as a single-degree-of-freedom damped free harmonic oscillator. Thus, for free oscillation, the governing equation of motion can be written as follows:

$$m_{\text{eff}}\ddot{x}(t) + c\dot{x}(t) + k_{\text{eff}}x(t) = 0 \tag{1}$$

where $x(t)$ is the displacement, m_{eff} is the effective mass, c is the damping constant, and k_{eff} is the effective spring constant. The effective stiffness k_{eff} $(=3E_RI/L^3)$ is the deflection at the end of the beam due to the unit load, and the effective mass m_{eff} $(=0.236$ m) is the concentrated mass located at the end of

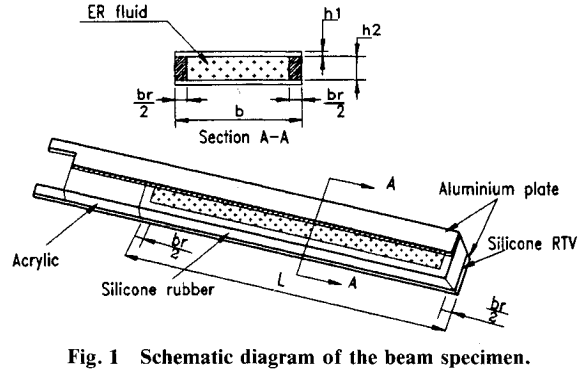

Fig. 1 Schematic diagram of the beam specimen.

Received July 27, 1992; revision received July 8, 1993; accepted for publication Aug. 11, 1993.

*Professor, Department of Mechanical Engineering.
†Graduate Student, Department of Mechanical Engineering.
‡Senior Researcher, Suspension Development and Dynamic Analysis Division.

Table 1 Specifications of the ER fluid and specimens

Specimen	A	B	C
Liquid, viscosity	Silicone oil, 50 cS	Silicone oil, 50 cS	Silicone oil, 50 cS
Particle	Cornstarch	Cornstarch	Cornstarch
Particle concentration, %	55	55	45
ER fluid volume fraction, %	52.3	45.3	52.3
L, mm	200	200	200
b, mm	20	20	20
br, mm	4	6	4
h1, mm	0.5	0.5	0.5
h2, mm	2	2	2

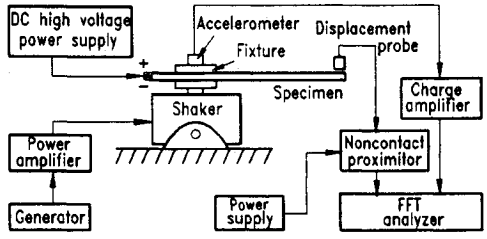

Fig. 2 Experimental setup.

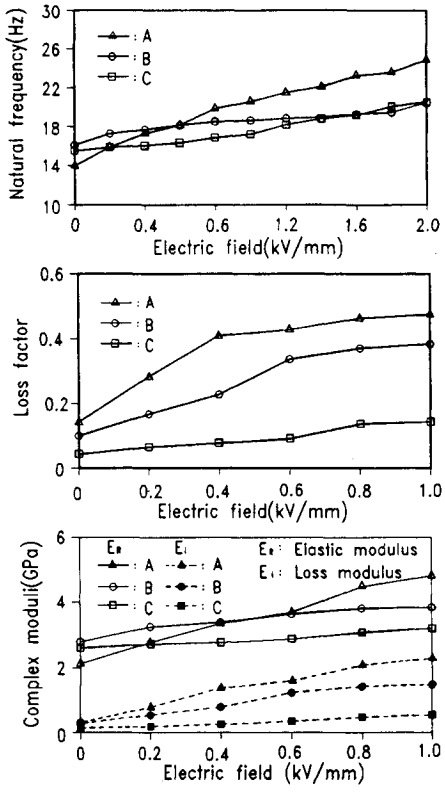

Fig. 3 Electric-field-dependent elastodynamic properties.

the beam needed to yield the same kinetic energy of oscillation as a beam with a total, uniformly distributed mass m. By considering this analogized harmonic oscillator, one can express the natural frequency in terms of the effective stiffness and mass as follows:

$$\omega_n = \sqrt{(k_{\text{eff}}/m_{\text{eff}})} = \sqrt{(3E_R I/L^3 m_{\text{eff}})} \tag{2}$$

The beam filled with the ER fluid acts as viscoelastic materials so that complex moduli can be expressed as follows:

$$E^* = E_R + iE_I, \qquad i = \sqrt{-1} \tag{3}$$

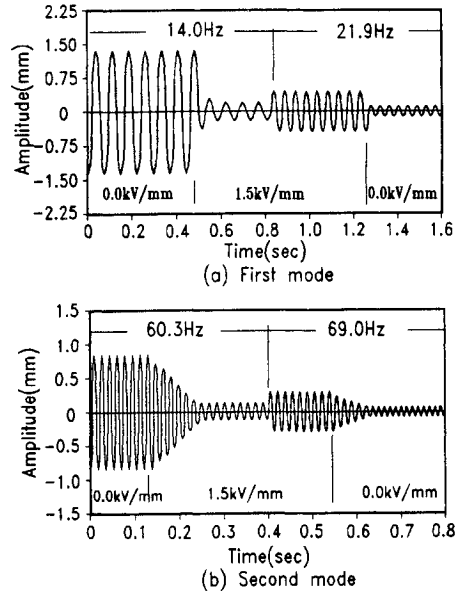

Fig. 4 Controllabilities of the beam A.

where E_R is the elastic (or storage) modulus and E_I is the loss modulus. The ratio of E_I to E_R was used to determine the following damping parameter:

$$E_I/E_R = \delta/\pi = \eta, \qquad \delta = \frac{1}{n}\ln(x_1/x_{n+1}) \tag{4}$$

where δ is the logarithmic decrement, η is the loss factor, and n is the number of decrements to the x_n oscillation peak; δ was measured by applying prescribed initial tip deflection to the beam.

Subsequently, from Eqs. (2) and (4), E_R and E_I were obtained. This analysis of E_R and E_I assumes that the beam specimen behaves in a uniform and isotropic manner. On the other hand, to examine the feasibility of using the ER fluid as an actuator in an active vibration control system, we measured the decrement of the amplitude and the transient period of the beam by applying the electric field in a manner of bang-off-bang control type.

Results and Discussions

Electric-field-dependent elastodynamic properties such as damped natural frequency (first mode), loss factor, and complex moduli are shown in Fig. 3. In the variations of the damped natural frequencies, it is clearly observed that the specimen A that has both greater volume fraction and concentration of the ER fluid gives the highest frequency increment, reaching up to 80% by employing the electric field of 2.0 kV/mm compared with that at 0 kV/mm, whereas the increments of the damped natural frequencies of the specimens B and C are about 30% with the same field strength. Therefore, in the case of using the ER fluid as an actuator for an active vibration control system, the specimen A produces wider control bandwidth than the specimens B and C. The frequencies increase in almost a linear fashion as the field strength increases. In the variations of the loss factor and complex moduli, it is observed that again the specimen A yields the highest increment. These results imply that the concentration of the ER fluid is a more important composition parameter than the volume fraction.

Figure 4 shows the controllability of the beam A under resonance conditions. The amplitudes (tip deflections) of the beam excited with the resonant frequencies of 14.0 Hz (first mode) and 60.3 Hz (second mode) at 0 kV/mm were reduced by 85 and 84% by applying the electric field of 1.5 kV/mm, respectively. The transient period was 0.14 s at the first mode and 0.15 s at the second mode. The magnitudes excited with the resonant frequencies of 21.9 and 69.0 Hz at 1.5 kV/mm

were also reduced by eliminating the field strength. These results advocate that the resonance of the beam can be avoided by employing the ER fluid as an actuator in the control system. It is finally noted that the derivation of phenomenological governing equations of the proposed smart structure using the data observed in this experimental investigation is yet to be further studied.

References

[1]Rogers, C. A., Baker, K. D., and Jaeger, C. A., "Introduction to Smart Materials and Structures," *Proceedings of the U. S. Army Workshop on Smart Materials, Structures, and Mathematical Issues* (Blacksburg, VA), 1988, pp. 17-28.

[2]Crawley, E. F., and De Luis, J., "Use of Piezoelectric Actuators as Elements of Intelligent Structures," *AIAA Journal*, Vol. 25, No. 10, 1987, pp. 1373-1385.

[3]Yaeger, J. R., "A Practical Shape Memory Electromechanical Actuator," *Proceedings of International Symposium on Automotive Technology and Automation* (Milan, Italy), Vol. 1, 1984, pp. 633-642.

[4]Gandhi, M. V., Thompson, B. S., and Choi, S. B., "A New Generation of Innovative Ultra-Advanced Intelligent Composite Materials Featuring Electro-Rheological Fluids: An Experimental Investigation," *Journal of Composite Materials*, Vol. 23, No. 12, 1989, pp. 1232-1255.

Determining Free-Free Modes from Experimental Data of Constrained Structures

Su-Huan Chen,* Zhong-Sheng Liu,†
Wan-Zhi Han,‡ and Ai-Jun Ma‡
Jilin University of Technology,
Changchun 130022, People's Republic of China

Introduction

IT is very difficult to determine the frequencies and mode shapes of an unconstrained structure with experimental methods. Przemieniecki, in his monograph,[1] used vibration test data of a structure to determine the frequencies and mode shapes of the same structure in a free-free state. However, Przemieniecki's method requires that all of the frequencies and mode shapes of the constrained structure be obtained from the vibration tests, which is very difficult for a large structure. The lower frequencies and corresponding mode shapes can easily be obtained with much more accuracy from the vibration tests of the constrained structure, whereas the higher frequencies and the corresponding mode shapes are difficult to obtain. Some low-frequency modes can be obtained, whereas the high-frequency modes are truncated.

In this Note, a method for improving Przemieniecki's method is presented that extends Przemieniecki's method to deal with the problem of modal truncation. This method is of importance in extracting the natural frequencies and mode shapes of unconstrained structures, such as aircraft, rockets, and satellites, etc., from the experimental data of the corresponding constrained structures.

Przemieniecki's Method

Consider an unconstrained structure as shown in Fig. 1. Assume that the displacements on the unconstrained structure are partitioned into U_x and U_y. Furthermore, we assume that vibration tests to determine frequencies and mode shapes can be performed while supporting the structure in such a manner that $U_y = 0$ and that all rigid-body degrees of freedom are excluded. As an example we may use a rocket attached to its launch pad, shown in Fig. 1. The displacements U_y will be those associated with the attachment points, whereas U_x will represent all of the remaining displacements, the number of which will depend on the idealization of the structure.[1]

According to Ref. 1, we get

$$\left(\begin{bmatrix} K_{xx} & K_{xy} \\ K_{yx} & K_{yy} \end{bmatrix} - \omega^2 \begin{bmatrix} K_{xx}\bar{P}_e\bar{\Omega}_e^{-2}\bar{P}_e^{-1} & M_{xy} \\ M_{yx} & M_{yy} \end{bmatrix} \right) \begin{bmatrix} q_x \\ q_y \end{bmatrix} = 0 \quad (1)$$

$$\bar{P}_e = [\bar{\Psi}_1, \bar{\Psi}_2, \ldots, \bar{\Psi}_m] \quad (2)$$

$$\bar{\Omega}_e^2 = \text{diag}[\bar{\omega}_1^2, \bar{\omega}_2^2, \ldots, \bar{\omega}_m^2] \quad (3)$$

where $\bar{\Psi}_1, \bar{\Psi}_2, \ldots, \bar{\Psi}_m$ are the mode shapes for the constrained system with $U_y = 0$ and $\bar{\omega}_1, \bar{\omega}_2, \ldots, \bar{\omega}_m$ are the associated frequencies.

Equation (1) can be used to determine the frequencies ω and modes $\{q_x^T\ q_y^T\}$ for the unconstrained structure. The stiffness matrices K_{xx}, K_{xy}, K_{yx}, and K_{yy} can be obtained from static tests on the constrained structure by first determining the influence coefficients for the directions of U_x with $U_y = 0$ and then deriving the required stiffness matrix. The modes $\bar{P}_e$ and frequencies $\bar{\Omega}_e$ are obtained from vibration tests, which allow us to determine the matrix product $K_{xx}\bar{P}_e\bar{\Omega}_e^{-2}\bar{P}_e^{-1}$; however, the submatrices M_{xy}, M_{yx}, and M_{yy} must be calculated, since no reliable direct experimental techniques are available to measure mass matrices. Alternatively, the structure can be supported in other locations and the vibration tests carried out to determine the remaining mass submatrices.[1]

Treatment of the Unavailable Modes

In the vibration tests, only the small number of lower frequencies and the associated mode shapes can be accurately and easily identified, whereas the higher frequencies and the associated mode shapes are difficult to identify accurately. Accordingly, the higher frequencies and the associated mode shapes are often unavailable. It can be seen that Przemieniecki's method cannot be implemented in the case of the higher frequencies and the corresponding mode shapes truncated, because the terms in Eq. (1) include the inverse of the modal matrix $\bar{P}_e^{-1}$, which requires all of the mode shapes. An approach to the modal truncation problem encountered in using Przemieniecki's method is presented in the following.

Let us focus on $K_{xx}\bar{P}_e\bar{\Omega}_e^{-2}\bar{P}_e^{-1}$. Set

$$W = K_{xx}\bar{P}_e\bar{\Omega}_e^{-2}\bar{P}_e^{-1} \quad (4)$$

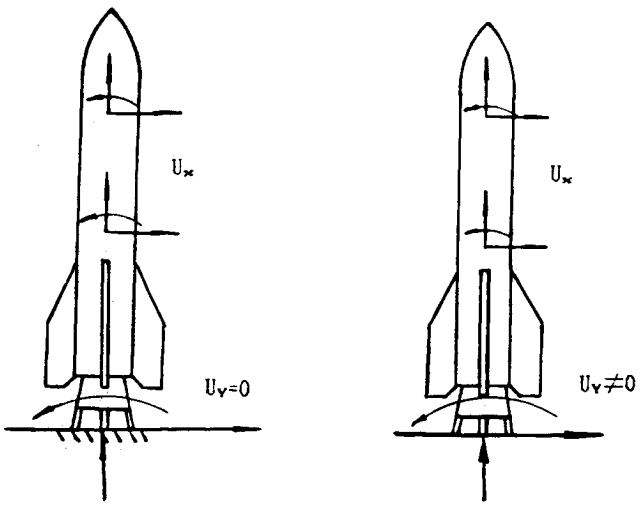

Fig. 1 Unconstrained structure.

Received Aug. 5, 1992; revision received Jan. 27, 1993; accepted for publication March 16, 1993.

*Professor, Department of Mechanics.
†Post-Doctoral Researcher, Department of Mechanics.
‡Ph.D. Student, Department of Mechanics.